NASA/TM—2015-218749

# A Fully Nonmetallic Gas Turbine Engine Enabled by Additive Manufacturing

## Part II: Additive Manufacturing and Characterization of Polymer Composites

*Kathy Chuang, Joseph E. Grady, Steve M. Arnold, and Robert D. Draper*
*Glenn Research Center, Cleveland, Ohio*

*Eugene Shin*
*Ohio Aerospace Institute, Brook Park, Ohio*

*Clark Patterson and Tom Santelle*
*Rapid Prototyping+Manufacturing (rp+m), Avon Lake, Ohio*

*Chao Lao, Morgan Rhein, and Jeremy Mehl*
*Glenn Research Center, Cleveland, Ohio*

June 2015

# NASA STI Program . . . in Profile

Since its founding, NASA has been dedicated to the advancement of aeronautics and space science. The NASA Scientific and Technical Information (STI) Program plays a key part in helping NASA maintain this important role.

The NASA STI Program operates under the auspices of the Agency Chief Information Officer. It collects, organizes, provides for archiving, and disseminates NASA's STI. The NASA STI Program provides access to the NASA Technical Report Server—Registered (NTRS Reg) and NASA Technical Report Server—Public (NTRS) thus providing one of the largest collections of aeronautical and space science STI in the world. Results are published in both non-NASA channels and by NASA in the NASA STI Report Series, which includes the following report types:

- TECHNICAL PUBLICATION. Reports of completed research or a major significant phase of research that present the results of NASA programs and include extensive data or theoretical analysis. Includes compilations of significant scientific and technical data and information deemed to be of continuing reference value. NASA counter-part of peer-reviewed formal professional papers, but has less stringent limitations on manuscript length and extent of graphic presentations.

- TECHNICAL MEMORANDUM. Scientific and technical findings that are preliminary or of specialized interest, e.g., "quick-release" reports, working papers, and bibliographies that contain minimal annotation. Does not contain extensive analysis.

- CONTRACTOR REPORT. Scientific and technical findings by NASA-sponsored contractors and grantees.

- CONFERENCE PUBLICATION. Collected papers from scientific and technical conferences, symposia, seminars, or other meetings sponsored or co-sponsored by NASA.

- SPECIAL PUBLICATION. Scientific, technical, or historical information from NASA programs, projects, and missions, often concerned with subjects having substantial public interest.

- TECHNICAL TRANSLATION. English-language translations of foreign scientific and technical material pertinent to NASA's mission.

For more information about the NASA STI program, see the following:

- Access the NASA STI program home page at http://www.sti.nasa.gov

- E-mail your question to help@sti.nasa.gov

- Fax your question to the NASA STI Information Desk at 757-864-6500

- Telephone the NASA STI Information Desk at 757-864-9658

- Write to:
  NASA STI Program
  Mail Stop 148
  NASA Langley Research Center
  Hampton, VA 23681-2199

NASA/TM—2015-218749

# A Fully Nonmetallic Gas Turbine Engine Enabled by Additive Manufacturing

## Part II: Additive Manufacturing and Characterization of Polymer Composites

*Kathy Chuang, Joseph E. Grady, Steve M. Arnold, and Robert D. Draper*
*Glenn Research Center, Cleveland, Ohio*

*Eugene Shin*
*Ohio Aerospace Institute, Brook Park, Ohio*

*Clark Patterson and Tom Santelle*
*Rapid Prototyping+Manufacturing (rp+m), Avon Lake, Ohio*

*Chao Lao, Morgan Rhein, and Jeremy Mehl*
*Glenn Research Center, Cleveland, Ohio*

National Aeronautics and
Space Administration

Glenn Research Center
Cleveland, Ohio 44135

June 2015

## Acknowledgments

The authors would like to thank Drs. Mike Dudley and Koushik Datta from NASA Aeronautics Research Institute for their continuous support and encouragements. In addition, we would like to thank Michael Vinup, Natalie Wali and Don Weir of Honeywell Aerospace for providing component CAD files, and the following collaborators for their contribution in terms of material characterization and mechanical testing efforts for this report: Pete Bonacuse, GRC-LMA, Joy Buehler/LMA-VPL, Chris Burke/LM-SLI, Chris Kantzos/GRC, LERCIP intern, Rich Martin/LMA-CSU, Linda McCorkle and Daniel Scheiman/ LMN-OAI, D. Jordan McCrone/ LMA-VPL, Bob Pelaez/GRC-FTH, Larry Smith/FTC-Jacobs, Tim Ubienski/FTH-SLI, Nathan Wilmoth/LMA-VPL and rp+m staffs.



*Level of Review*: This material has been technically reviewed by technical management.

Available from

NASA STI Program
Mail Stop 148
NASA Langley Research Center
Hampton, VA 23681-2199

National Technical Information Service
5285 Port Royal Road
Springfield, VA 22161
703-605-6000

This report is available in electronic form at http://www.sti.nasa.gov/ and http://ntrs.nasa.gov/

# A Fully Nonmetallic Gas Turbine Engine Enabled by Additive Manufacturing

## Part II: Additive Manufacturing and Characterization of Polymer Composites

Kathy Chuang, Joseph E. Grady, Steve M. Arnold, and Robert D. Draper
National Aeronautics and Space Administration
Glenn Research Center
Cleveland, Ohio 44135

Eugene Shin
Ohio Aerospace Institute
Brook Park, Ohio 44142

Clark Patterson and Tom Santelle
Rapid Prototype Plus Manufacturing (rp+m)
Avon Lake, Ohio 44012

Chao Lao,* Morgan Rhein,* and Jeremy Mehl*
National Aeronautics and Space Administration
Glenn Research Center
Cleveland, Ohio 44135

## Abstract

This publication is the second part of the three part report of the project entitled "A Fully Nonmetallic Gas Turbine Engine Enabled by Additive Manufacturing" funded by NASA Aeronautics Research Institute (NARI). The objective of this project was to conduct additive manufacturing to produce aircraft engine components by Fused Deposition Modeling (FDM), using commercially available polyetherimides—Ultem 9085 and experimental Ultem 1000 mixed with 10% chopped carbon fiber. A property comparison between FDM-printed and injection molded coupons for Ultem 9085, Ultem 1000 resin and the fiber-filled composite Ultem 1000 was carried out. Furthermore, an acoustic liner was printed from Ultem 9085 simulating conventional honeycomb structured liners and tested in a wind tunnel. Composite compressor inlet guide vanes were also printed using fiber-filled Ultem 1000 filaments and tested in a cascade rig. The fiber-filled Ultem 1000 filaments and composite vanes were characterized by scanning electron microscope (SEM) and acid digestion to determine the porosity of FDM-printed articles which ranged from 25 to 31%. Coupons of Ultem 9085, experimental Ultem 1000 composites and XH6050 resin were tested at room temperature and 400 °F to evaluate their corresponding mechanical properties. A preliminary modeling was also initiated to predict the mechanical properties of FDM-printed Ultem 9085 coupons in relation to varied raster angles and void contents, using the GRC-developed MAC/GMC program.

## 1. Introduction

Additive manufacturing (AM) has gained considerable attention recently, because of the promise of being able to produce net shape 3D components layer by layer directly by automated machines. This is especially true for complex shape polymer parts and low production volume components, which are not

*NASA Glenn Research Center, academy intern 2014.

economical to produce by injection molding. In addition, AM offers quick turn-around time for specialty parts and shortened production and testing cycle for components. This project concentrated on Fused Deposition Modeling (FDM) technique (Fig. 1) in which a polymer filament is melted and then deposited in successive layers to build a 3D component according to a computer-aided design (CAD) file (Ref. 1). The state-of-the art of FDM are populated with commercial acrylonitrile butadiene styrene (ABS), polycarbonate (Ref. 2) and polyamides such as Nylons for use as prototyping at the temperature around 100 to 125 °C (212 to 257 °F).

One objective of the project was to develop additive manufacturing approaches for polymeric aircraft engine components and conduct testing on coupons as well as built parts, such as acoustic testing in a wind tunnel. The Ultem 9085 polyetherimide filament is one of the commercial polymers marketed by Stratasys for use in FDM with a glass transition temperature ($T_g$) of 186 °C (367 °F). Ultem 9085 is certified by FAA as flame retardant polymer for use in aircraft cabin. This project used Ultem 9085 as the baseline polymer for printing demonstration components, such as acoustic liners and a perforated engine access door. Furthermore, this project also strived to advance the FDM process into building polymer composites for aircraft engine parts. These additively manufactured components were tested in rigs and results have been presented in the first part of the report (Ref. 3). The Ultem 1000 with 10% AS4 carbon fiber was chosen as the candidate fiber-filled polymer filaments for this project, because Stratasys is making it available for the first time as an experimental filament under the State funded Ohio Third Frontier research project. Ultem 1000 is a homopolymer with higher $T_g$ (217 °C, 423 °F) than that of Ultem 9085 which is a blend of polycarbonate and Ultem 1000 with lower viscosity and cost suitable for injection molding.

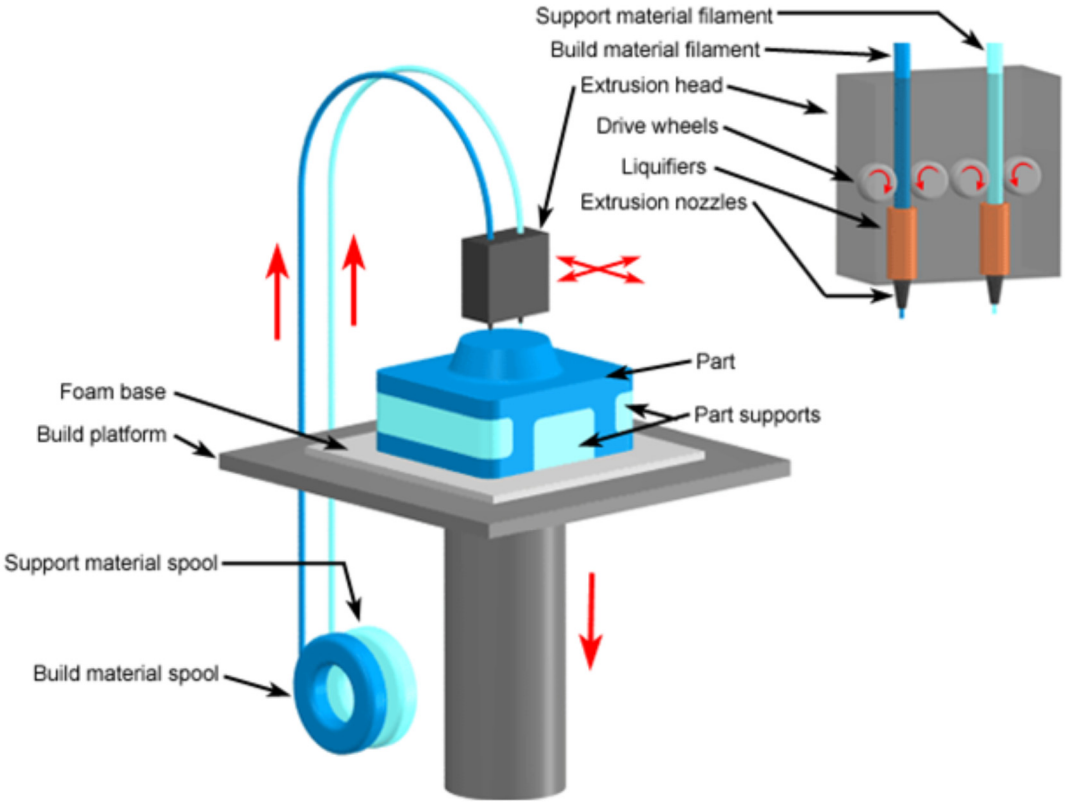


Figure 1.—Schematic of Fused Deposition Modeling (FDM) process.

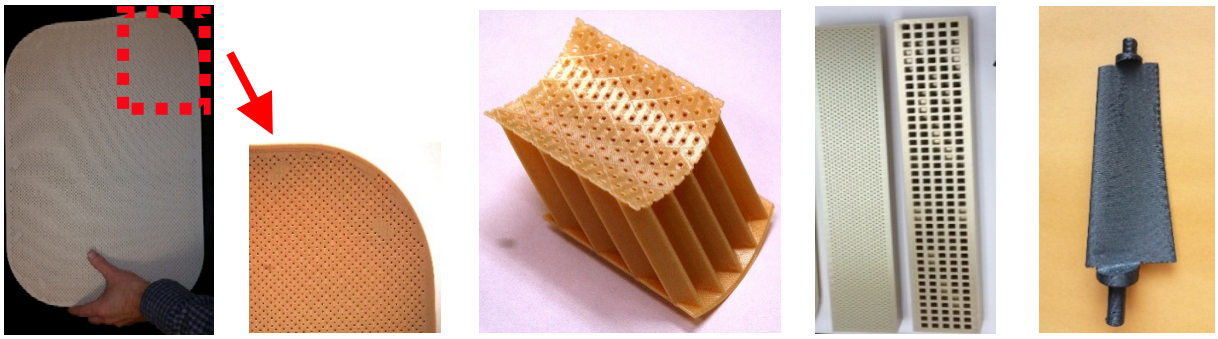

(a) Perforated engine access door (Ultem 9085)

(b) Acoustic liner and components (Ultem 9085)

(c) Composite vanes Ultem 1000/fiber

Figure 2.—FDM printed polymer components.

## 2. Experimental

All the FDM printing was performed at Rapid Prototype Plus Manufacturing (rp+m), using Stratasys' open source Fortus 400 or 900 mc FDM machines. The experimental XH6050 resin and carbon-fiber-filled Ultem 1000 filaments were supplied by Stratasys under the Ohio Third Frontier Program—Advanced Materials for Additive Manufacturing Maturation. The Ultem resins and composites were printed between 375 to 420 °C (707 to 788 °F). The specific engine components were selected by Honeywell Aerospace. Using Ultem 9085, a perforated engine door (Fig. 2(a)), an acoustic liner and its demonstration components (Fig. 2(b)) with 93 °C (200 °F) use temperature were printed by FDM at 375 °C in one piece, simulating the Aramid honeycomb structures bonded with epoxy composite face sheet. Additionally, composite vanes (Fig. 2(c)) with use temperature up to 204 °C (400 °F) were printed at 420 °C, using Ultem 1000 filled with 10% chopped AS4 carbon fibers. Rig testing conditions and results of acoustic liner and composite inlet guide vane (IGV) are described in details in the first part of the report (Ref. 3).

## 3. Results and Discussion

### 3.1 Property Comparison of FDM and Injection Molding

A mechanical property comparison between FDM-printed and injection-molded coupons of Ultem 9085, Ultem 1000 and the carbon-fiber-filled Ultem 1000 are shown in Table 1. These data indicated that Ultem 9085 (printed at 0° raster angle), displayed about 87% of tensile strength and 64% of modulus, as compared to the injection molded counter parts, due to the presence of inherent porosities within the FDM-printed test coupons. The porosity of FDM-printed Ultem 9085 was about 5 to 8%, depending on the orientation of the layup. The mechanical strength of FDM generated specimens also relied on the built direction, the thickness of the filaments, the tool path generation and the air gap between raster in the filled pattern. In general, the FDM generated structures are more brittle and have lower elongation than the injection molded counterparts (Ref. 4).

### 3.2 Initial Characterization of Carbon Fiber Filled Ultem 1000 Composites and Filaments

The initial tensile strength of 10% AS4 fiber-filled Ultem 1000 composites (first batch ever made from Stratasys) was only about 70% of Ultem 9085 resin as printed by FDM (Fig. 3), which was much lower than expected. The printing of ±45° raster angle reduced the strength by 80 to 86% as opposed to 0°. Further investigation by acid digestion indicated that the porosity of fiber-filler Ultem 1000 vanes are unusually high, ranging from 23 to 26% (Table 2). The printing orientation did not exhibit much difference in terms of porosity. However, the porosity measurement based on the integration of optical microscope images (Fig. 4) ranged from 29 to 34% (Table 3), which was even higher than the 23 to 26% porosity obtained by acid digestion.

TABLE 1.—PROPERTY COMPARISON OF ULTEM 9085 AND ULTEM 1000 BY INJECTION MOLDING *VS* FDM

| esin type<br><br>Properties | Ultem 9085 injection molded (Sabic data) | Ultem 9085 FDM printed (Stratasys data) 0° | Ultem 9085 FDM rp+m (GRC tested) ±45° | Ultem 1000 injection molded (Sabic data) | Ultem 1000+10 wt% AS4 chopped C-fiber FDM rp+m (GRC tested) 0°/±45° |
|---|---|---|---|---|---|
| Tensile strength (MPa) | 83 | 72 | 62±0.1 | 110 | 50±0.9/44±0.3 |
| Tensile modulus (MPa) | 3,432 | 2,200 | 2,230±12 | 3,579 | 2,901±48/2248±46 |
| Flexural strength (MPa) | 137 | 115 | 92±2 | 165 | tbd |
| Flexural modulus (MPa) | 2,913 | 2,500 | 1,901±41 | 3,511 | tbd |
| Compression strength (MPa) | n/a | 104 | tbd | n/a | tbd |
| Compression modulus (MPa) | n/a | 1,930 | 1,890±32 | n/a | tbd |

*No Ultem 1000 filament for FDM is commercially available.

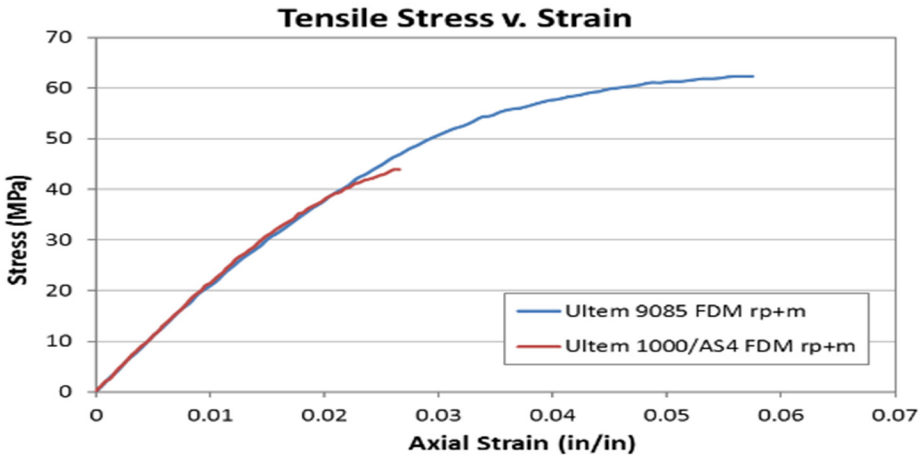


Figure 3.—Tensile properties of Ultem 9085 and fiber-filled Ultem 1000 as received.

TABLE 2.—POROSITY OF FIBER-FILLED ULTEM 1000 COMPOSITE VANES BY ACID DIGESTION

| Sample ID | After drying | | | | | From Theor. Density | | | | FWF | FVF | porosity |
|---|---|---|---|---|---|---|---|---|---|---|---|---|
| | Balance | Pycnometer | | Acid digestion | | | | | | | | |
| | Mc, g | Vc, cc | ρc, g/cc | Mf, g | Mm, g | Vf, cc | Vm, cc | Vp, cc | Vp, cc | wt% | v% | v% |
| Ha1 | 0.7731 | 0.831 | 0.931 | 0.0712 | 0.702 | 0.0398 | 0.5527 | 0.2376 | 0.2385 | 9% | 5% | 28.7% |
| Ha2 | 0.3977 | 0.374 | 1.063 | 0.0498 | 0.348 | 0.0278 | 0.2739 | 0.0720 | 0.0722 | 13% | 7% | 19.3% |
| Ha3 | 0.9433 | 0.952 | 0.992 | 0.0894 | 0.854 | 0.0499 | 0.6724 | 0.2300 | 0.2297 | 9% | 5% | 24.1% |
| Ha4 | 0.6676 | 0.734 | 0.911 | 0.0753 | 0.592 | 0.0421 | 0.4664 | 0.2252 | 0.2256 | 11% | 6% | 30.7% |
| Ha5 | 1.1184 | 1.194 | 0.939 | 0.0627 | 1.056 | 0.0350 | 0.8313 | 0.3279 | 0.3277 | 6% | 3% | 27.4% |
| ***Avg*** | | | | | | | | | | ***10% ±3*** | ***5% ±2*** | ***26% ±4*** |
| Va1 | 0.8706 | 0.929 | 0.938 | n/a | | | | | | | | |
| Va2 | 0.3349 | 0.347 | 0.966 | 0.0346 | 0.300 | 0.0193 | 0.2365 | 0.0911 | 0.0912 | 10% | 6% | 26.29% |
| Va3 | 0.5443 | 0.492 | 1.112 | 0.0413 | 0.503 | 0.0231 | 0.3961 | 0.0727 | 0.0729 | 8% | 5% | 14.81% |
| Va4 | 0.637 | 0.695 | 0.92 | 0.0632 | 0.574 | 0.0353 | 0.4518 | 0.2064 | 0.2079 | 10% | 5% | 29.91% |
| Va5 | 1.2997 | 1.25 | 1.037 | 0.0833 | 1.216 | 0.0465 | 0.9578 | 0.2462 | 0.2457 | 6% | 4% | 19.65% |
| ***Avg*** | | | | | | | | | | ***9% ±2*** | ***5% ±1*** | ***23% ±7*** |

TABLE 3.—POROSITY OF COMPOSITE VANES BASED ON OPTICAL MICROSCOPE IMAGES

| Sample ID | Average* ± S.D. | | Sample ID | Average* ± S.D. | |
|---|---|---|---|---|---|
| | FVF, v% | Porosity, v% | | FVF, v% | Porosity, v% |
| Hmy1 | 5.7% ± 0.3% | 33.2% ± 0.3% | Vmy1 | 7.5% ± 0.3% | 29.9% ± 2.6% |
| Hmy4 | 5.0% ± 0.3% | 34.8% ± 1.7% | Vmy5 | 7.3% ± 0.6% | 32.5% ± 5.0% |
| Hmy5 | 6.4% ± 0.3% | 32.3% ± 1.5% | Vmz1 | 5.1% ± 0.3% | 39.2% ± 1.6% |
| Hmz1 | 7.1% ± 0.3% | 33.4% ± 3.2% | Vmz3 | 6.8% ± 0.4% | 31.2% ± 2.8% |
| Hmz3 | 6.8% ± 0.6% | 33.3% ± 5.2% | Vmz4 | 7.0% ± 0.3% | 33.8% ± 0.8% |
| Hmz4 | 7.5% ± 0.4% | 28.9% ± 3.8% | Vmz5 | 6.5% ± 0.4% | 31.6% ± 2.4% |
| Hmz5 | 6.3% ± 0.4% | 34.4% ± 3.0% | | | |
| **Overall Avg ± SD** | **6.4% ± 0.7%** | **33.2% ± 3.2%** | **Overall Avg ± SD** | **6.7% ± 0.8%** | **32.9% ± 4.1%** |

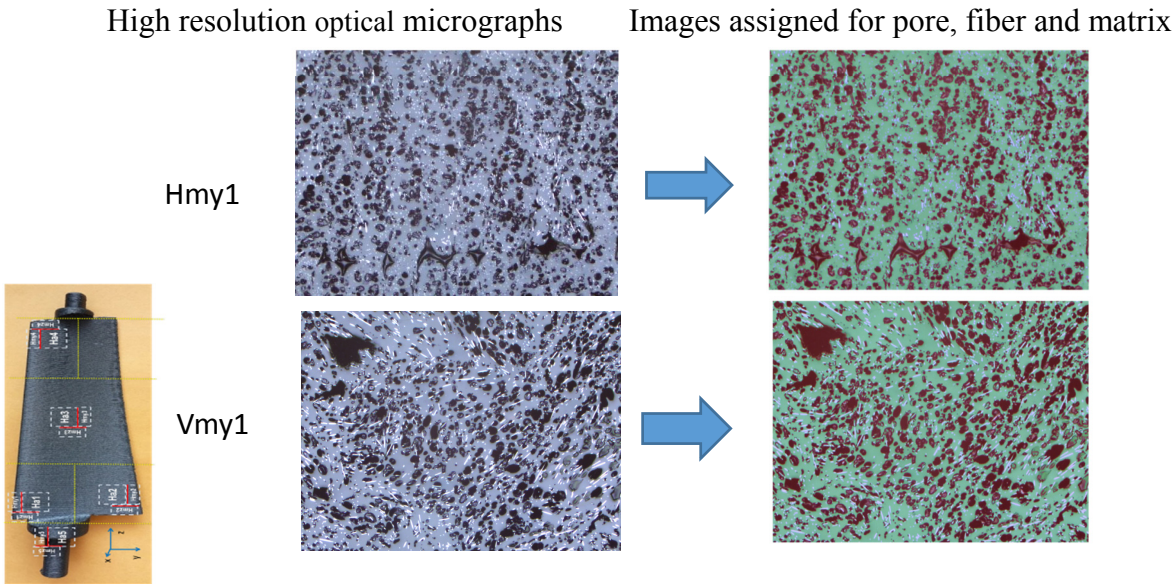


Figure 4.—High resolution of optical micrographs (left) and images of pore, fiber and matrix (right) of a FDM-printed composite vane.

To understand the origin of high porosity in the FDM-printed fiber-filled Ultem 1000 composites, an effort was initiated to investigate the as-received thick Ultem 1000 filament filled with 10% chopped AS4 carbon fibers, which was fed into the FDM machine. The fiber-filled Ultem 1000 filaments were produced by mixing 6 mm AS4 chopped fibers with Ultem 1000 in an extruder, cut into pellets, and then re-extruded into filaments at Stratasys. As shown in Figure 5, the longitudinal section (a) revealed that the chopped fibers were aligned with the filament axis, and significant amounts of the fibers were further chopped into average length of 2 to 3 mm during the extrusion process. The cross section (b) to (e) indicated that there were little voids present in the as-received filaments in this segment of initial investigation.

Separately, thin filaments of fiber-filled Ultem 1000 extruded from the liquefier of Stratasys' Fortus 400 mc FDM machine at 420 °C were collected and analyzed, since these thin filaments were used directly for FDM printing. As shown in Figure 6, the FDM extruded thin filaments were full of voids in the form of blisters, due to the sudden exposure to extreme high heat.

The acid digestion values in Table 4 confirmed that this segment of as-received thick fiber-filled filament analyzed had no porosity as confirmed by the photomicrographs in Figure 5. The fiber content was 9% by weight which was very close to the original formulation of 10% chopped fibers. However, the thin FDM-extruded filaments were found to have about 31% of porosity, which was closer to the image analysis result of 33% porosity than that of 24 to 26% porosity by acid digestion of the printed vane.

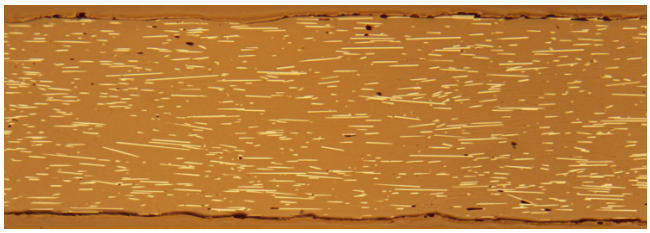

(a) Longitudinal section of fiber filled filament

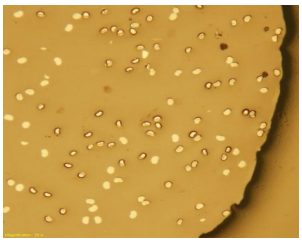

(b) Cross section

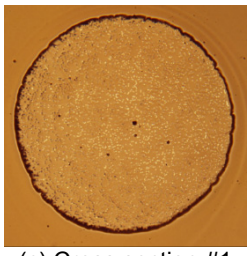

(c) Cross section #1

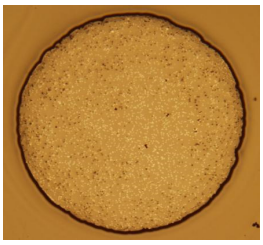

(d) Cross section #2
after removing ~1 mm

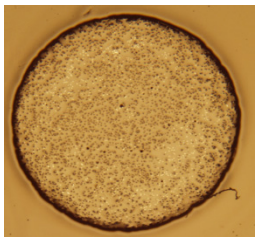

(e) Cross section #3
after removing ~2 mm

Figure 5.—Photomicrographs of 10% AS4 fiber filled Ultem 1000 filaments (as received-thick).

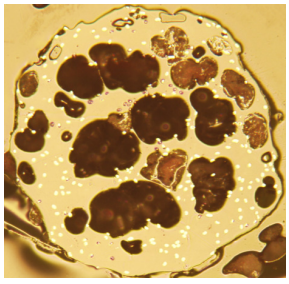

(a) Cross section#1

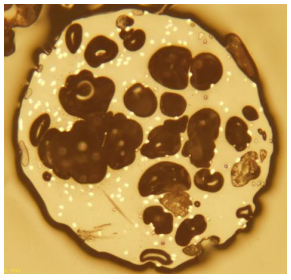

(b) Cross section #2
after removing ~1 mm

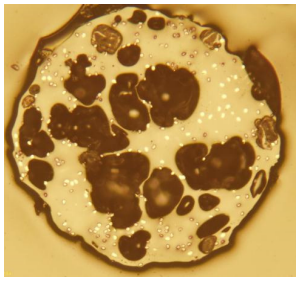

(c) Cross section #3
after removing ~2 mm

Figure 6.—Photomicrographs of 10% AS4 fiber filled Ultem 1000 filaments (FDM-extruded-thin).

TABLE 4.—POROSITY OF FIBER-FILLED ULTEM 1000 FILAMENTS

| Sample ID | After drying | | | | | From Theor. Density | | | FWF, wt% | FVF, v% | porosity, v% |
|---|---|---|---|---|---|---|---|---|---|---|---|
| | Balance | Pycnometer | | Acid digestion | | | | | | | |
| | Mc, g | Vc, cc | ρc, g/cc | Mf, g | Mm, g | Vf, cc | Vm, cc | Vp, cc | | | |
| **Filament, thick** | 0.2753 | 0.2084 | 1.3209 | 0.0254 | 0.250 | 0.014 | 0.1968 | -0.003 | **9%** | **7%** | **-1.2%** |
| **Filament, thin 1** | 0.0582 | 0.0645 | 0.9029 | 0.0054 | 0.053 | 0.003 | 0.0416 | 0.02 | **9%** | **5%** | **30.9%** |
| **thin 2** | 0.0583 | 0.0653 | 0.8924 | 0.0054 | 0.053 | 0.003 | 0.0417 | 0.021 | **9%** | **5%** | **31.6%** |

*Thick filament—as received and fed into FDM machine; thin filament—extruded from FDM machine.

Thermogravimetric analysis (TGA) with Fourier Transform Infrared Spectroscopy (FTIR) was carried out to investigate the origin of blistering. As shown in Figure 7, the major weight loss shown in TGA up to 300 °C (572 °F) corresponded to water shown in FTIR, which indicated that some water was trapped inside the filament, which was more difficult to remove than the surface water. Additionally, Figure 8 indicated that Ultem 1000 resin pellet contained 0.375% of water, and the fiber-filled Ultem 1000 filament had 0.593% of water whereas separate TGA analysis had indicated that the chopped fiber contained 0.25% of water. These two curves indicated that other than water loss, the Ultem resin and filament are very stable until about 500 °C (932 °F). However, the thin fiber-filled filament showed not only the loss of surface water around 100 °C (212 °F), but also some other weight loss due to degradation, as it had been exposed to the sudden high temperature of 420 °C (788 °F) at the liquefier in the FDM machine during the melting process. This first lot of the fiber-filled Ultem 1000 filament seemed to be solid but brittle whereas the thin filament appeared to be fragile and extremely porous.

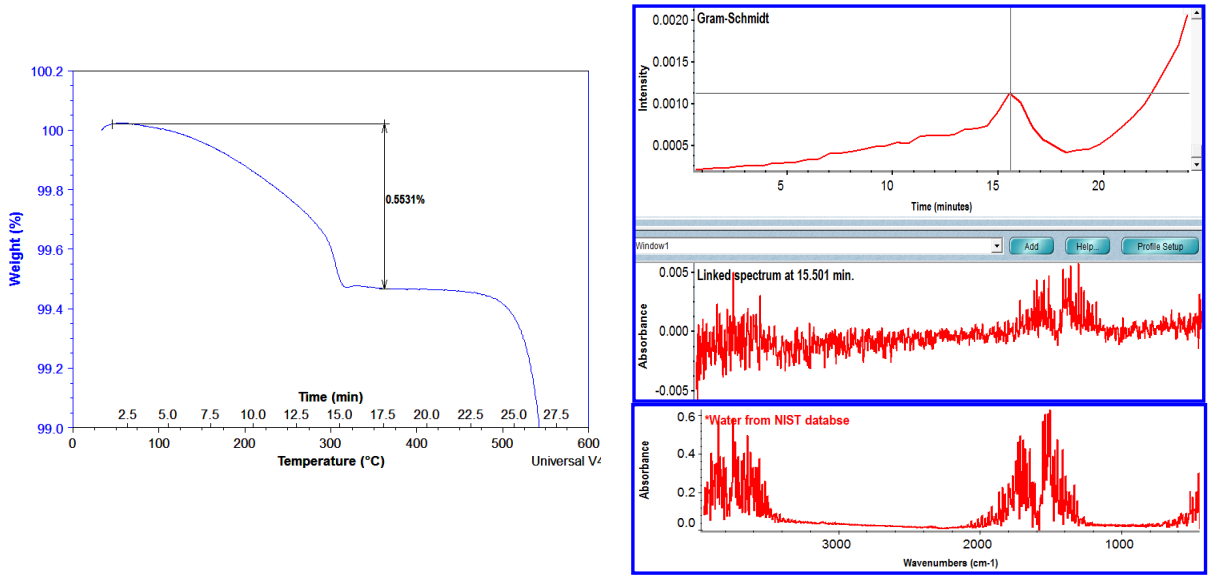


Figure 7.—TGA-FTIR analysis of the fiber-filled Ultem 1000 filament.

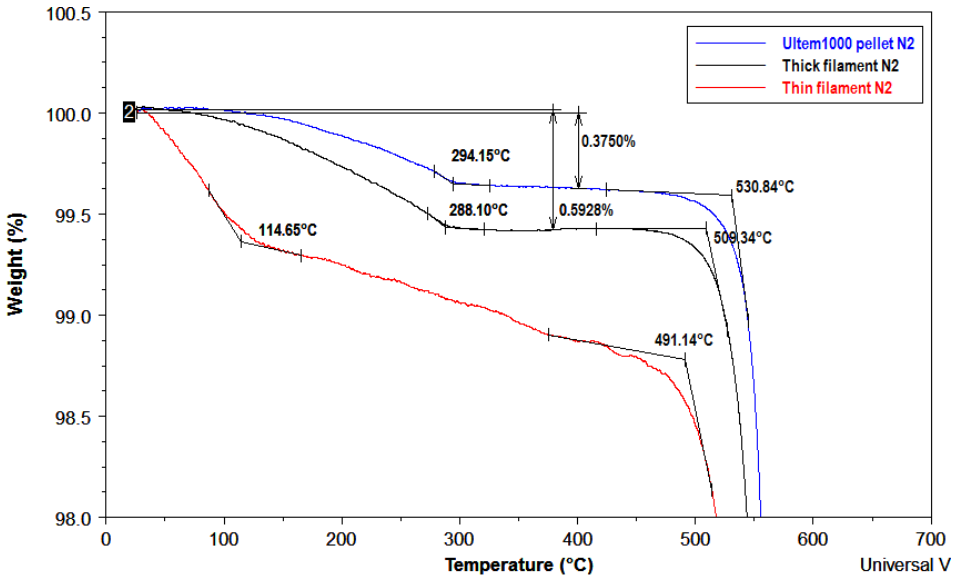


Figure 8.—Thermogravimetric analysis of and fiber-filled Ultem 1000 filament and resin pellet.

### 3.3 Development and Evaluation of Drying Processes for Fiber-Filled Ultem 1000 Filaments

(1) To improve the quality and mechanical properties of FDM-printed composites, an initial drying of as-received filament at 185 °C (365 °F) was carried out to remove the water from fiber-filled Ultem 1000 in an air-circulation oven for 12 hr; this was followed by the printing two cubes by FDM (Fig. 9). The dried thick filaments and FDM-spun thin fibers seemed shrunken and more ductile than the corresponding as-received filaments and un-dried FDM-spun thin filaments. The resulting printed cubes contained much lower porosity (13.6 to 17.4%) than that of the vanes (23 to 26%) as indicted in Table 2.

(2) A second drying trial for fiber-filled Ultem 1000 was conducted at 204 °C (400 °F) for 22 hr. SEM micrographs in Figure 10 showed that the dried thick filaments still had large pores of voids which were formed by the trapped water, air or other gases within the filaments during extrusion and drying (Fig. 10(a)), as well as the small pores of fiber pull-out at the fracture surface. Furthermore, Figure 10(b) revealed that the porosity of FDM-spun thin filaments was much higher than the thick filaments as confirmed by acid digestion values listed in Table 5. The severe porosity of thin filaments were the results of volume expansion of trapped water vapors, air bubbles or other gases generated from the degradation of Ultem 1000 resin exposed to the sudden high liquefying temperature of 420 °C (788 °F) used to spin it within the FDM machine.

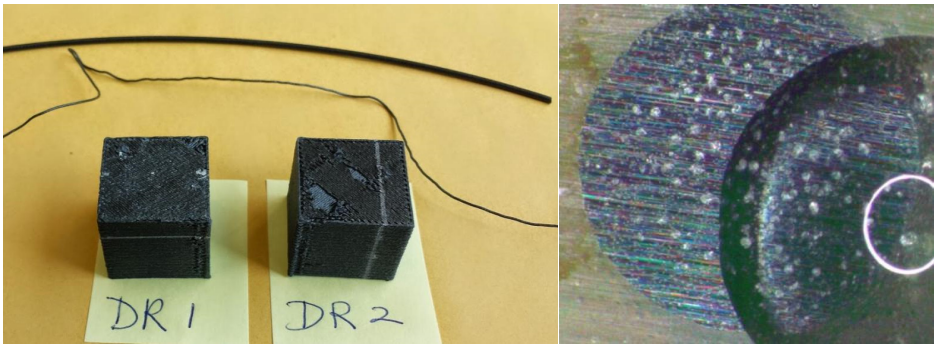


Figure 9.—Picture and micrograph of fiber-filled Ultem 1000 filaments and printed cubes.

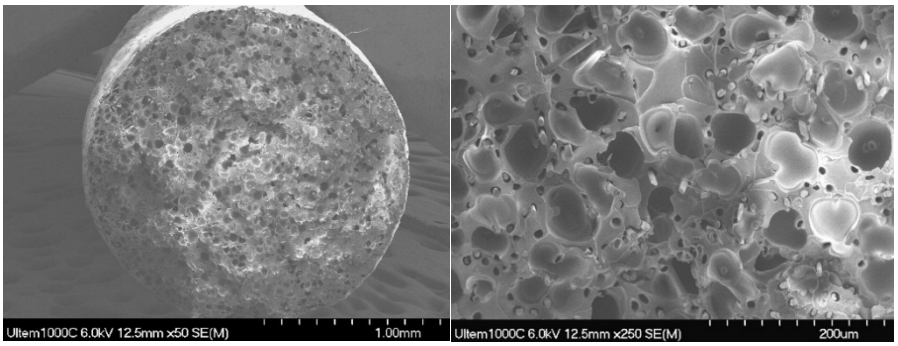


(a) Thick filament after drying at 204 °C (400 °F) for 22 hr

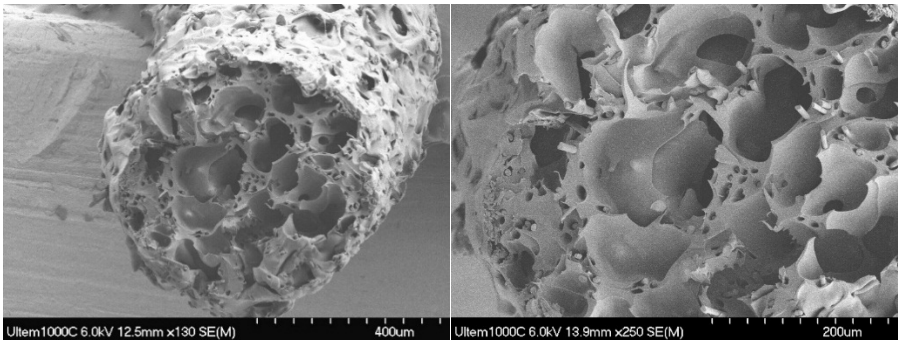


(b) FDM-spun thin filaments derived from 204 °C dried thick filaments

Figure 10.—SEM of fiber-filled Ultem 1000 filament after drying at 204 °C for 22 hr.

(3) A third drying process was conducted in a desiccant system at 149 °C (300 °F) for 12 hr and characterized along with another section of as-received thick carbon-filled Ultem 1000 filaments as a repeat to investigate the uniformity and porosity of the experimental composite filaments supplied by Stratasys. As shown in Table 5, the porosity of the fiber-filled Ultem 1000 thick filaments as-received for the second trial was 15.3% which is much higher than the void-free in the initial as-received filaments. This clearly indicated that the porosity of experimental fiber-filled Ultem 1000 filaments varied considerably from 0 to 15.3%, and the porosity remained at 15% even after drying at 149 °C for 12 hr (Fig. 11). The photomicrographs in Figure 10 confirmed that as-received fiber-filled Ultem 1000 filaments exhibited some porosity this time, in contrast to the void-free segment shown in Figure 4 previously. Since the moisture content of the as-received Ultem 1000 composite filaments was only 0.6%, including 0.2% moisture from as-received chopped fibers, the voids shown in the as-received fiber-filled Ultem 1000 thick filaments could either come from moisture trapped inside or the air bubbles introduced during the extrusion process. Nevertheless, after drying at various conditions, all the FDM-extruded thin filaments still displayed consistent porosity of ~25%, which is similar to porosity of printed composite vanes, but lower than the 30% porosity detected in the FDM-extruded thin filaments derived from the undried thick filaments (Table 5). This fact clearly indicated that once the moisture pore or air bubbles formed within the filaments, they are much more difficult to remove than surface water.

TABLE 5.—POROSITY OF VARIOUS DRIED FIBER-FILLED ULTEM 1000 FILAMENTS

| Sample ID | FWF, wt% | FVF, v% | Porosity,v% |
|---|---|---|---|
| **1st Gen Composite Vanes (received @ 6/18/14)** | | | |
| ***Horizontal Vane*** | *9.6%* | *5.2%* | *26.1%* |
| ***Vertical Vane*** | *8.6%* | *4.8%* | *22.7%* |
| ***As-rec Filament, thick*** | 9.2% | 6.8% | -1.2% |
| ***FDM extruded, thin*** | 9.3% | 4.7% | 30.9% |
| **185 °C dried filament and cubes (samples received @ 8/25/14)** | | | |
| ***As-dried Filament, thick*** | 10.1% | 6.7% | 8.5% |
| ***Dried & extruded, thin*** | 10.0% | 5.3% | 28.3% |
| ***DR1 Cube*** | 9.6% | 6.0% | 13.6% |
| ***DR2 Cube*** | 9.5% | 5.7% | 17.4% |
| **204.4 °C ( 400 °F) dried filament (samples received @ 10/17/14)** | | | |
| ***As-dried Filament, thick*** | 8.5% | 5.2% | 16.5% |
| ***Dried & extruded, thin*** | 5.2% | 2.8% | 24.5% |
| **149 °C (300 °F) dried filaments but in a desiccant system, received @ 12/8/14** | | | |
| ***As-received from Stratasys*** | 9.6% | 5.9% | 15.3% |
| ***As-dried Filament, thick*** | 9.5% | 5.9% | 15.0% |
| ***Dried & extruded, thin*** | 10.2% | 5.5% | 25.6% |

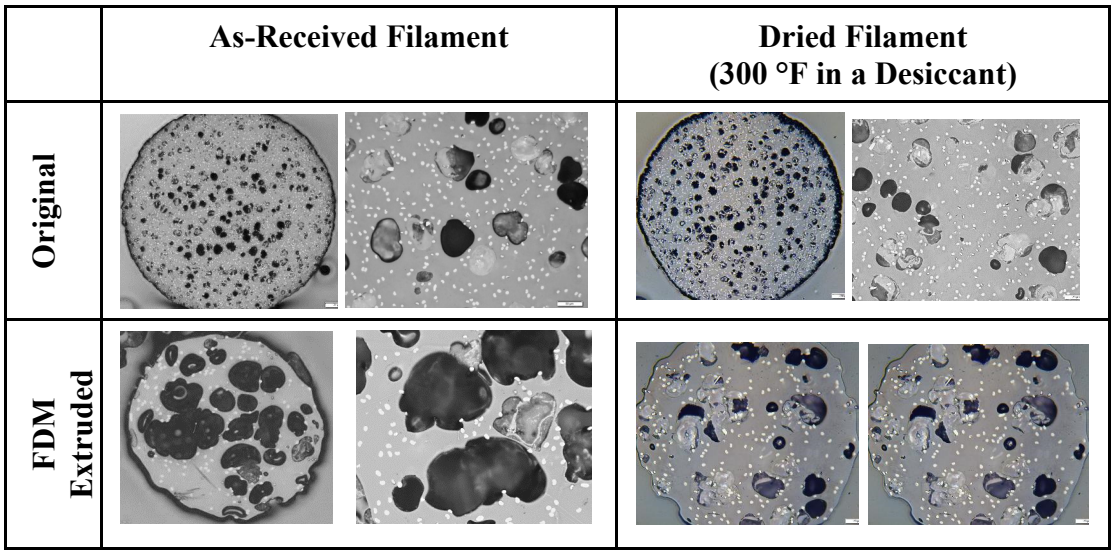


Figure 11.—Optical Micrographs of as-received and dried fiber-filled Ultem 1000 filaments.

### 3.4 Mechanical Properties of FDM-Printed Ultem Resins and Fiber-Filled Ultem 1000

Tensile tests of FDM-printed Ultem 9085, Ultem 1000, XH6050 and fiber-filled Ultem 1000 coupons were conducted at room temperature and 204 °C (400 °F) as listed in Table 6. Figure 12 showed that Ultem 1000/C-fiber composite printed with the dried FDM filament showed the highest modulus while Ultem 9085 resin showed the highest toughness and strength at room temperature. The carbon fiber reinforcement Ultem 1000 was estimated to increase the tensile strength by 23% and modulus by 38% while the strain-to-failure ration dropped by 55%, back-calculated based on XH6050 data of injection-molded versus FDM-printed. Regardless of test temperature, Ultem XH6050 showed inferior properties than either Ultem 1000 composites or Ultem 9085 ($T_g$ = 186 °C), despite of its higher $T_g$ (245 °C). XH6050 also showed significant losses in toughness and strength at 204 °C (400 °F). Thermal analysis results in Table 7 showed that substantial moisture still trapped within the composites even after drying.

More specifically, drying FDM filament prior to FDM-printing improved the room temperature (RT) properties of Ultem 1000 composites considerably, as indicated by the reduced porosities of FDM-extruded thin filaments from 30 to 24% after various drying conditions (Table 5), especially ±45° samples, even though its residual moisture content was still high. As shown in Figure 13, the 0° sample, showed ~8% increase in modulus, ~3% increase in strength, but ~11% decrease in strain-to-failure. The ±45° sample displayed ~26% increase in modulus, ~20% increase in strength, but ~2.4% decrease in strain-to-failure. At 204 °C which is near Ultem1000's $T_g$ (217 °C), all the properties decreased considerably due to the softening of the resin.

TABLE 6.—MECHANICAL PROPERTIES OF ULTEM 9085, ULTEM 1000, XH6500, FIBER-FILLER ULTEM 1000

| Material | Process | Printing Orientation | Tensile Properties at RT (23 °C) | | | | |
|---|---|---|---|---|---|---|---|
| | | | Modulus MPa | Strength MPa | Strain-to-Failure, % | Poisson's Ratio | Data Source |
| **ULTEM 9085** | Injection Molded | n/a | 3,432 ± n/a | 83 ± n/a | 72 ± n/a | n/a ± | Sabic |
| | FDM by Stratasys | 0° | 2,200 ± n/a | 72 ± n/a | 6.0 ± n/a | n/a ± | Stratasys |
| | FDM by rp+m | ± 45° | 2,230 ± 12 | 62 ± 0.1 | 6.1 ± 0.4 | 0.38 ± 0.02 | GRC |
| **ULTEM 1000** | Injection Molded | n/a | 3,579 ± n/a | 110 ± n/a | 60 ± n/a | n/a ± | Sabic |
| **ULTEM 1000 + 10wt% AS4 C-fiber: As-received filament** | FDM by rp+m | 0° | 2,901 ± 48 | 50 ± 0.9 | 2.4 ± 0.1 | 0.33 ± 0.01 | GRC* |
| | FDM by rp+m | ± 45° | 2,248 ± 46 | 44 ± 0.3 | 2.8 ± 0.1 | 0.39 ± 0.01 | GRC* |
| **ULTEM 1000 + 10wt% AS4 C-fiber: Dried filament at 300°F** | FDM by rp+m | 0° | 3,132 ± 20 | 52 ± 2.0 | 2.1 ± 0.0 | 0.35 ± 0.02 | GRC* |
| | FDM by rp+m | ± 45° | 2,835 ± 177 | 53 ± 1.8 | 2.7 ± 0.1 | 0.34 ± 0.02 | GRC* |
| **ULTEM XH6050** | Injection Molded | n/a | 3,511 ± n/a | 96 ± n/a | 25 ± n/a | n/a ± | Sabic |
| | FDM by rp+m | 0° | 2,069 ± 190 | 36 ± 4.7 | 2.2 ± 0.3 | 0.33 ± 0 | GRC* |
| | FDM by rp+m | ± 45° | 1,938 ± 105 | 35 ± 4.8 | 2.2 ± 0.5 | 0.38 ± 0 | GRC* |
| | | | Tensile Properties at 400 °F (204 °C) | | | | |
| **ULTEM 1000 + 10wt% AS4 C-fiber: As-received filament** | FDM by rp+m | 0° | 1,920 ± 94 | 11.4 ± 0.5 | 5.2 ± 3.4 | 0.32 ± 0.08 | GRC* |
| | FDM by rp+m | ± 45° | 1,456 ± 143 | 9.3 ± 0.5 | 5.2 ± 3.7 | 0.33 ± 0.04 | GRC* |
| **ULTEM 1000 + 10wt% AS4 C-fiber: Dried filament at 300°F** | FDM by rp+m | 0° | 1,951 ± 119 | 11.4 ± 1.3 | 9.2 ± 3.7 | 0.30 ± 0.06 | GRC* |
| | FDM by rp+m | ± 45° | 1,197 ± 82 | 5.8 ± 2.3 | 43.5 ± 7.8 | 0.35 ± 0.03 | GRC* |
| **ULTEM XH6050** | FDM by rp+m | 0° | 1,497 ± 26 | 9.4 ± 0.6 | 0.65 ± 0.1 | 0.34 ± 0.1 | GRC* |
| | FDM by rp+m | ± 45° | 1,367 ± 123 | 8.2 ± 1.1 | 0.6 ± 0.1 | 0.41 ± 0.1 | GRC* |

** All GRC testing used 0.2 in/min CHS and averaged out of three repeat runs.*

*No Ultem 1000 filament for FDM is commercially available

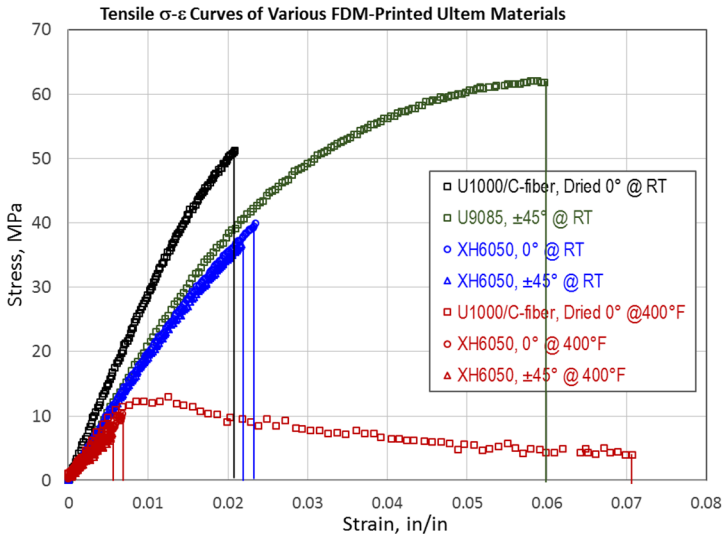


Figure 12.—Tensile properties of FDM-printed Ultem resins and fiber-filled Ultem 1000.

TABLE 7.—THERMAL ANALYSIS OF FIBER-FILLED ULTEM 1000 COMPOSITES

| Sample ID | mDSC Tg, °C | | TGA (under N2 gas) | | | | |
|---|---|---|---|---|---|---|---|
| | Total Heat | Rev. Heat | Td, °C | ΔWt% RT-100 °C | ΔWt% 100 - 300 °C | ΔWt% @ 750 °C | Char yield |
| **1st Gen Composite Vanes (received @ 6/18/14)** | | | | | | | |
| Horizonal vane, top | 214 | 217 | 556 | 0.298 | 0.389 | 42 | 58 |
| Horizonal vane, bottom | 213 | 213 | 560 | 0.326 | 0.340 | 42 | 58 |
| Vertical vane, top | 213 | 217 | 558 | 0.332 | 0.303 | 42 | 58 |
| Vertical vane, bottom | 213 | 217 | 556 | 0.261 | 0.479 | 41 | 59 |
| ***As-received Filament*** | | | 563 | 0.074 | 0.580 | 40 | 60 |
| ***FDM-spun Filament*** | | | 550 | 0.500 | 0.574 | 40 | 60 |
| **185°C dried filament and cubes (samples received @ 8/25/14)** | | | | | | | |
| ***As-dried Filament*** | 214 | 217 | 563 | 0.110 | 0.471 | 41 | 60 |
| ***FDM-spun Filament*** | 213 | 215 | 560 | 0.403 | 0.178 | 37 | 63 |
| ***DR 1*** | 213 | 216 | 559 | 0.325 | 0.078 | 44 | 56 |
| **204.4 °C (400 °F) dried filament (samples received @ 10/17/14)** | | | | | | | |
| ***As-dried Filament*** | | | 565 | 0.050 | 0.199 | 43 | 57 |
| ***FDM-spun Filament*** | | | 557 | 0.313 | 0.387 | 43 | 57 |
| **149 °C (300 °F) dried filaments but in a desiccant system, received @ 12/8/14** | | | | | | | |
| ***As-received Filament*** | 215 | 220 | 554 | 0.094 | 0.331 | 42.5 | 57.5 |
| ***As-dried Filament*** | 214 | 216 | 554 | 0.062 | 0.374 | 42.2 | 57.8 |
| ***As-dried & extruded*** | | 215 | 546 | 0.154 | 0.438 | 45.9 | 54.1 |

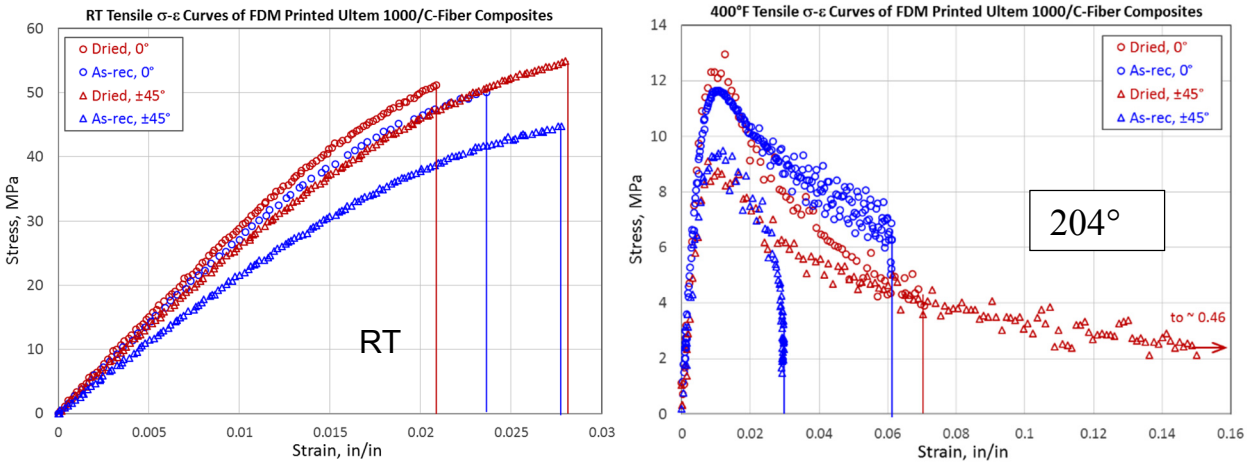


Figure 13.—Tensile properties of as-received and dried fiber-filled Ultem 1000 composites.

## 3.5 Characterization of Ultem 9085 and XH6050 Neat Resin Filaments

A detailed characterization effort was undertaken to understand why FDM-printed fiber-filled Ultem 1000 composites exhibited an average of 25% porosity whereas Ultem 9085 exhibited only 5 to 8% porosity due to inherent FDM process. Acid digestion of as-received Ultem 9085 neat resin filaments showed 1.8 to 3.5% porosity while XH6050 had none, but registered negative porosity because of errors in small quantity analysis (Table 8). In contrast, optical micrograms in Figure 14 indicated that both as-received Ultem 9085 filaments and thin filaments extruded at 375 °C by FDM exhibited no porosity. However, optical microscope image of the thin XH6050 filaments extruded at 410 °C by FDM revealed substantial voids due to blistering, but no porosity in the as-received thick filaments. The discrepancy of two methods depends on the segments of the filaments analyzed in each technique, and subjected to variable porosity. Compared to low porosity of neat resin filaments such as Ultem 9085 and XH6050, the fiber-filled Ultem 1000 composite filaments with varied porosity of 0 to 15% clearly warranted more process improvement. Thermal analysis (Table 9) of Ultem 9085 and XH6050 revealed that there were 0.3 to 0.4% weight loss between 100 to 300 °C due to moisture presence in these two resin filaments as received, which are common among all the moisture sensitive polyetherimides.

TABLE 8.—ANALYSIS OF ULTEM 9085 AND XH6050 RESIN FILAMENTS BY ACID DIGESTION

| Sample ID | Sample conditions | Drying | | Mass (g) | Pycnometer | Density (g/cc) | Porosity (%) |
|---|---|---|---|---|---|---|---|
| | | T (°C) | t (hr) | | Volume (cc) | | |
| Ultem 9085 | As-received Filament | 120 | 24 | 0.3972 | 0.302 | 1.3152 | 1.85 |
| | | 165 | 24 | 0.3963 | 0.3066 | 1.2926 | 3.54 |
| | Extruded Filament | 120 | 24 | 0.0743 | 0.0505 | 1.4713 | –9.80 |
| | | 165 | 24 | 0.0742 | 0.0506 | 1.4664 | –9.43 |
| Ultem XH6050 | As-received Filament | 120 | 24 | 0.3353 | 0.2492 | 1.3455 | –3.50 |
| | | 165 | 24 | 0.3356 | 0.249 | 1.3478 | –3.68 |
| | Extruded Filament | 120 | 24 | 0.1021 | 0.0766 | 1.3329 | –2.53 |
| | | 165 | 24 | 0.1024 | 0.0764 | 1.3403 | –3.10 |

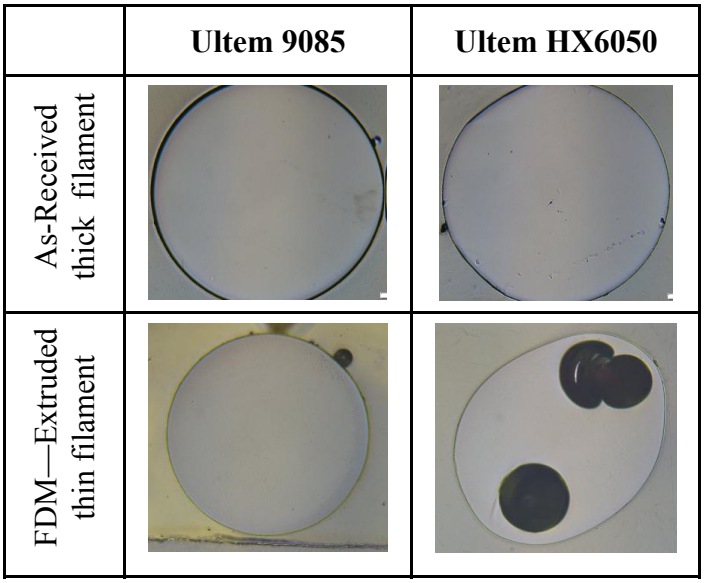


Figure 14.—Optical micrographs of Ultem 9085 and XH6050 resin filaments.

TABLE 9.—THERMAL ANALYSIS OF ULTEM 9085 AND XH6050

| Sample types | | mDSC Tg, °C | | TGA | | | |
|---|---|---|---|---|---|---|---|
| | | Total Heat | Rev. Heat | Td, °C | ΔWt% RT-100 °C | ΔWt% 100-300°C | ΔWt% @ 750 °C |
| **Ultem 9085** | ***Neat resin (manufacturer data)*** | | 186 | | | | |
| | ***As-received filament*** | 181 | 183 | 501 | 0.02044 | 0.3307 | 53 |
| | ***As-received and extruded filament*** | 177 | 184 | 501 | 0.09342 | 0.6288 | 55 |
| **Ultem XH6050** | ***Neat resin (manufacturer data)*** | | 247 | | | | |
| | ***As-received filament*** | 243 | 246 | 554 | 0.1116 | 0.4376 | 48 |
| | ***As-received and extruded filament*** | | 244 | 556 | 0.06844 | 0.1781 | 54 |

*mDSC stands for modulated Differential Scanning Calorimetry (DSC).

### 3.6 Computational Modeling of 3D Printing of Ultem 9085 by FDM

The object of this effort is to develop numerical models for generation of mesostructure of the printed product to account for the voids, raster angles of each layer that are inherently associated with the FDM process. The immediate goal is to enable the prediction of mechanical properties based on void contents and raster angles; however, the ultimate goal seeks to predict mechanical performance of the FDM printed components.

Modeling of Fused Deposition was performed using MAC/GMC program developed by Dr. Steven Arnold et al., at NASA Glenn for general composite applications. The repeat unit cell is shown in red in Figure 15.

In order to predict ultimate tensile stress of a specific material with corresponding parameters, such as varying raster angle and void percentage, the "failure sub-cell" capability was added and implemented in the MAC/GMC input file. The model utilizes user-defined material properties, such as $E_A$, $E_T$, $V_A$, $V_T$, $G_A$, CTE, and K, to compute the outcome according to desired orientation of the raster angle. It enables user to define limitation by either providing stress, strain, or both level where ultimate tensile stress occurs. Using known experimental strain data, the model is able to define the strain criteria for both materials in the axial load direction. During execution, the MAC/GMC code attempts to match user-defined failure criteria on each iteration. If the criteria are met, the code execution comes to a halt. Otherwise, it continues until the criteria are met or matches the defined iteration number. To incorporate another capability to the MAC/GMC model for the materials of interest, an adjustment was made to the input file for the Ultem 9085 model. After re-evaluating the model, and revised simulated thermo loading, the error between the calculated and experimental Young's modulus decreased drastically.

For example, different FDM print orientations were compared to injection molding processed Ultem 9085 while maintaining the same void amount for each orientation. Furthermore, mechanical and thermal loadings were implemented via the code to obtain tensile responses of each raster angle. Figure 16 showed the results of tensile response of Ultem 9085 at 135 °C, flat built with axial loading.

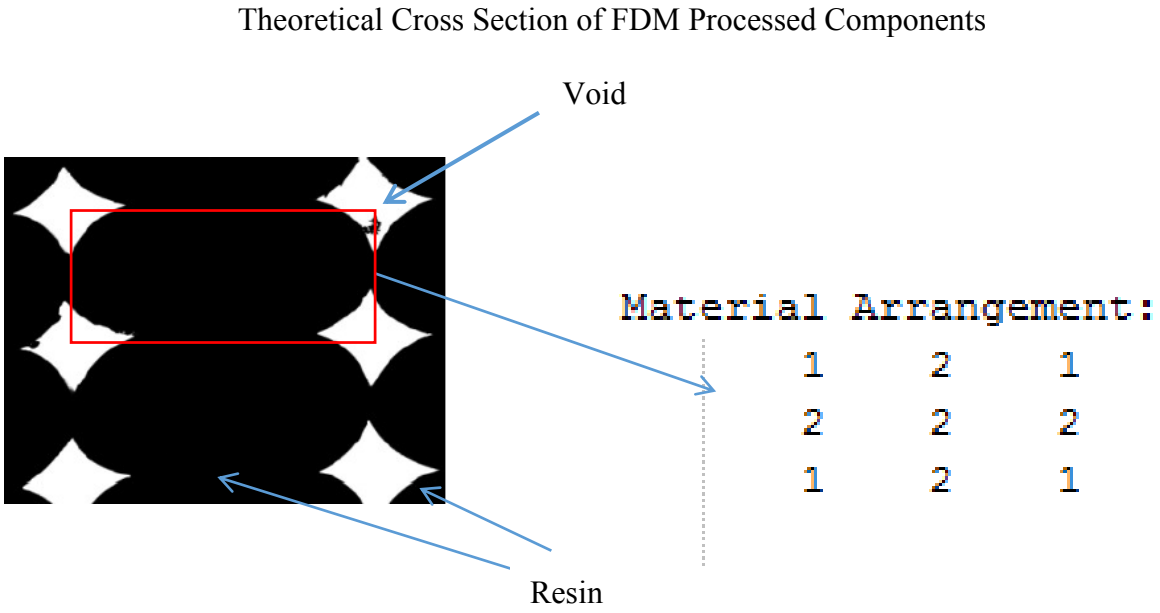


Figure 15.—Unit cell of 3D printing by FDM (Ref. 5).

The simulated data of Tables 10 to 14 and Figures 17 to 20 continue to show interesting optimal mechanical properties at the ±15° raster angle for Ultem 9085 and fiber filled Ultem 1000 composites and should be investigated further. As America Makes already collected a comprehensive database under contract on b-based allowable for FDM-printed Ultem 9085 specimens. Conceivably, one would be able to develop modeling techniques for FDM process that can be verified with the experimental mechanical data such as Ultem 9085. Hopefully, the computational modeling will one day be expanded into real capability for predicting performance of FDM printed parts.

TABLE 10.—CALCULATED TENSILE MODULUS OF INJECTION MOLDING PROCESSED MATERIALS

| 100% density | | |
|---|---|---|
| Materials | Tensile modulus (Gpa) | Tensile strength (Mpa) |
| Ultem 9085 | 1.72 | 83.83 |
| Ultem 1000 composite | 25.1 | 493.21 |

*Simulated at 135 °C.

TABLE 11.—CALCULATED TENSILE MODULUS OF ULTEM 9085 NEAT RESIN AT VARIED DENSITY AND RASTER

| Tensile modulus (Gpa) | | | | | |
|---|---|---|---|---|---|
| Raster angles | 96% density | 92% density | 85% density | 75% density | 70% density |
| 0/90° | 1.66 | 1.56 | 1.38 | 1.10 | 0.95 |
| ±15° | 1.65 | 1.59 | 1.44 | 1.21 | 1.09 |
| ±30° | 1.64 | 1.53 | 1.33 | 1.03 | 0.87 |
| ±45° | 1.62 | 1.49 | 1.25 | 0.90 | 0.73 |
| ±70° | 1.62 | 1.48 | 1.25 | 0.90 | 0.72 |

*Simulated loading speed 5 mm/min at 135 °C.

TABLE 12.—CALCULATED TENSILE MODULUS OF ULTEM 9085 RESIN AT VARIED DENSITY AND RASTER ANGLE

| Ultimate tensile strength (Mpa) | | | | | |
|---|---|---|---|---|---|
| Raster angles | 96% density | 92% density | 85% density | 75% density | 70% density |
| 0/90° | 78.79 | 73.79 | 65.08 | 50.46 | 42.05 |
| ±15° | 77.94 | 76.42 | 70.00 | 59.97 | 54.54 |
| ±30° | 79.17 | 74.35 | 65.86 | 51.79 | 43.68 |
| ±45° | 77.59 | 71.07 | 60.27 | 43.50 | 35.18 |
| ±70° | 77.66 | 71.70 | 61.20 | 44.07 | 35.41 |

*Simulated loading speed 5 mm/min at 135 °C.

TABLE 13.—CALCULATED TENSILE MODULUS OF ULTEM 1000 COMPOSITE AT VARIED DENSITY AND RASTER

| Tensile modulus (Gpa) | | | | | |
|---|---|---|---|---|---|
| Raster angles | 96% density | 92% density | 85% density | 75% density | 70% density |
| 0/90° | 8.76 | 8.28 | 8.06 | 7.43 | 6.64 |
| ±15° | 15.89 | 15.03 | 14.92 | 14.02 | 12.54 |
| ±30° | 7.69 | 7.27 | 6.99 | 6.34 | 5.67 |
| ±45° | 4.14 | 4.14 | 3.61 | 3.12 | 2.78 |
| ±70° | 3.13 | 2.96 | 2.67 | 2.26 | 2.01 |

*Simulated loading speed 5 mm/min at 204 °C.

TABLE 14.—CALCULATED TENSILE MODULUS OF ULTEM 1000 COMPOSITE AT VARIED DENSITY AND RASTER ANGLE

| Ultimate tensile strength (Mpa) | | | | | |
|---|---|---|---|---|---|
| Raster angles | 96% density | 92% density | 85% density | 75% density | 70% density |
| 0/90° | 170.18 | 161.17 | 156.72 | 145.19 | 129.95 |
| ±15° | 276.08 | 271.84 | 257.36 | 241.19 | 216.10 |
| ±30° | 174.74 | 166.35 | 161.65 | 136.50 | 124.22 |
| ±45° | 89.74 | 83.97 | 73.78 | 59.95 | 49.04 |
| ±70° | 83.11 | 77.85 | 68.11 | 55.66 | 53.31 |

*Simulated loading speed 5 mm/min at 204 °C.

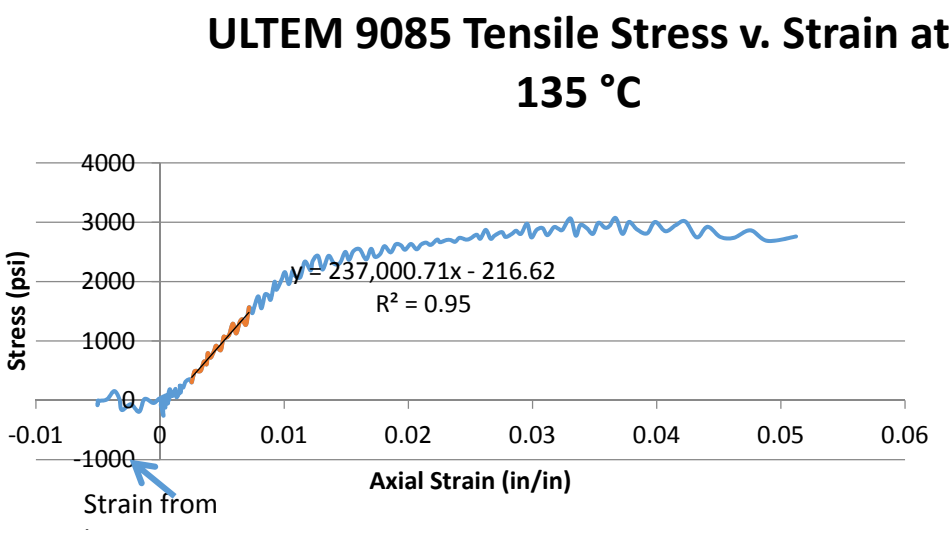


Figure 16.—Modeling of Ultem 9085 tensile properties.

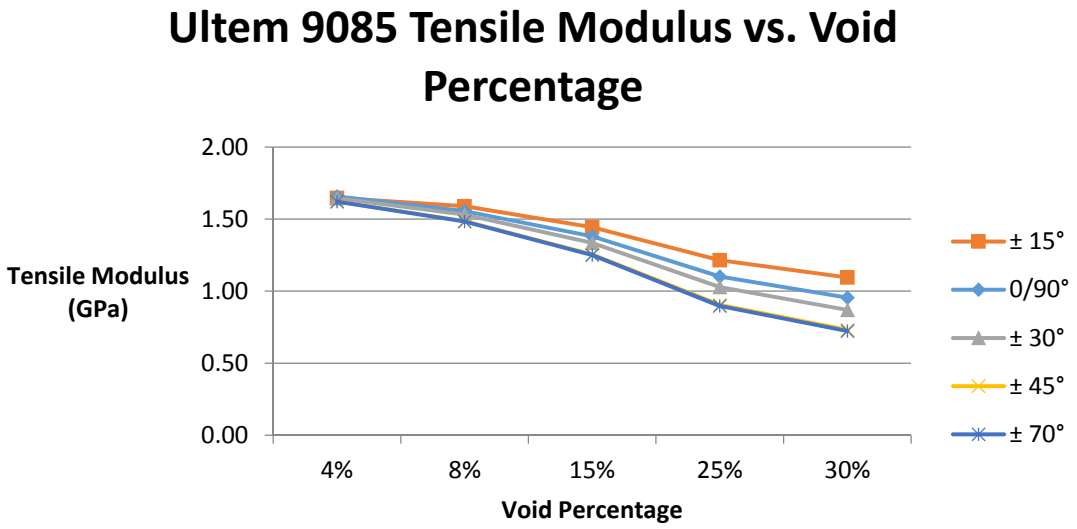


Figure 17.—Tensile modulus at different void percentage in a specimen.

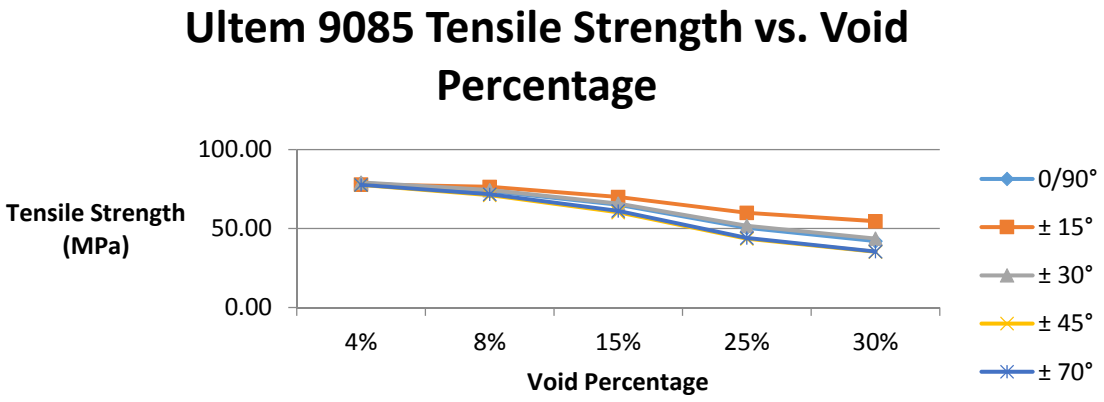


Figure 18.—Ultimate tensile strength at different void percentage in a sample.

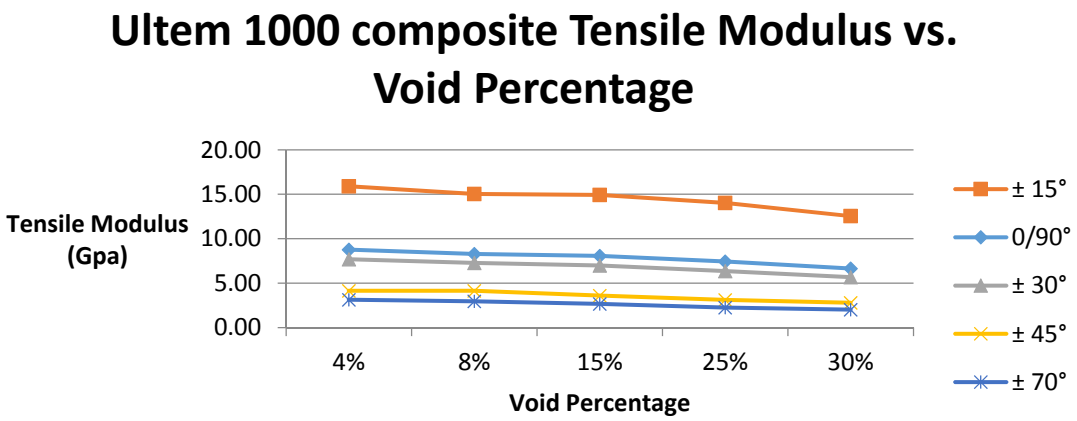


Figure 19.—Void percent versus tensile modulus for Ultem 1000 composite.

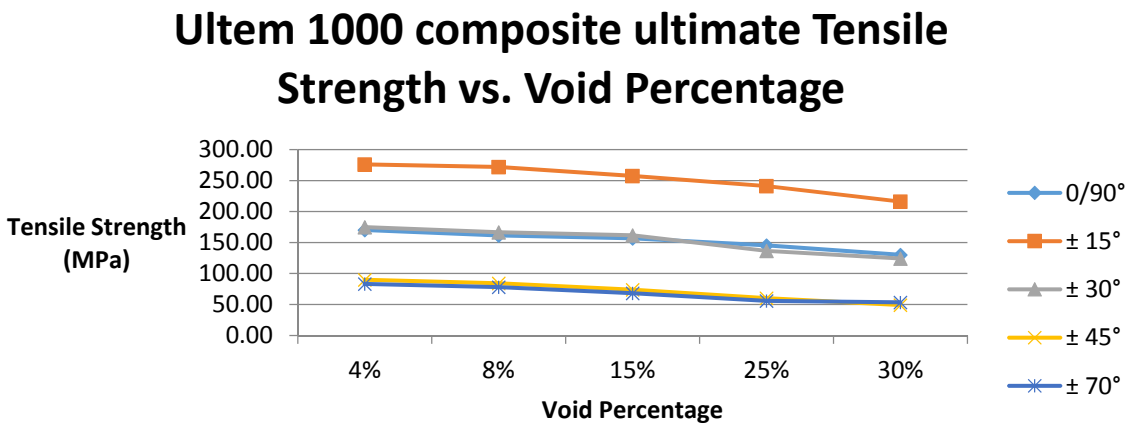


Figure 20.—Trend for void percentage versus ultimate tensile strength for Ultem 1000 composites.

## 4 Summary and Conclusions

To advance the state-of-the-art in additive manufacturing via Fused Deposition Modeling (FDM) beyond the commonly used ABS, polycarbonate and Nylons as prototyping for 100 to 125 °C use, this project aimed at producing aircraft engine components by FDM, using Ultem 9085 and cabon fiber-filled Ultem 1000 composite filaments with higher temperature (130 to 175 °C) capability.

A perforated access engine door and acoustic liners simulating conventional honeycomb structures, were printed with Ultem 9085 to modulate the sound wave and reduce noises. Composite engine inlet guide vanes were printed using Ultem 1000 filled with 10% AS4 chopped fibers as a reinforcement to eliminate the need for machining when using conventional polymer prepregs to make vanes. Preliminary data indicated that the FDM-printed Ultem 9085 exhibited about 84% of its original strength and 64 percent of its original modulus compared to its injection-molded counter parts. The incorporation of 10% chopped fiber into Ultem 1000 increased the tensile strength by 23% and modulus by 38%, but also made the resulting composites more brittle. The experimental fiber-filled Ultem 1000 filaments (as received) contained 0 to 15% varied porosity. However, the FDM extruded thin filaments and FDM printed Ultem 1000 composite vanes exhibited ~25% porosity, due to the volume expansion of trapped moisture, air or other gases generated form degradation at elevated printing temperature of 420 °C by FDM. In contrast, the

Ultem 9085 resin filament is a high quality commercial product that manufactures 3D objects with 5 to 8% porosity inherently associated with the FDM process, when printing at 375 °C. The tensile properties of the new experimental Ultem XH6050 FDM resin is inferior to Ultem 9085, even though its $T_g$ is roughly 60 °C higher than that of Ultem 9085.

In summary, this project proved the feasibility of printing integrated complex aircraft parts with polymers by FDM. FDM printing compared favorable to bonded honeycomb structures with face sheets in acoustic liners. However, printing composite parts by FDM is still considered experimental, as in the case of this effort to print Ultem 1000 composite vanes. Incorporation of 10% of chopped fibers into Ultem 1000 raised the viscosity significantly that affected the compounding efficiency in the extruder, resulting in high porosity in the extruded filaments and FDM-printed composite objects. In light of conventional polymer composites with 65% fiber content, additive manufacturing only looks favorable for printing intricate parts that are difficult to manufacture by conventional methods. In order to increase the fiber content and reduce porosity in polymer composites, it might be worthwhile to look into printing composite structures using thermoset polyimides with higher temperature performance and lower viscosity by selective laser sintering (SLS) for future works. The modeling of the FDM process using Ultem 9085 was intended to correlate the mechanical performance of FDM-printed objects with void contents and variation with different raster angles within each layer using GRC-developed MAX/GMC program for composites. The rough matching between mechanical test results and modeling prediction in this brief work is encouraging. Recent establishment of b-based allowable of Ultem 9085 in America Makes' contract report as an industrial database (Ref. 6) offers an excellent opportunity to verify computer modeling with mechanical properties of FDM-printed test coupons. The ultimate goal to predict the performance of FDM-printed parts by computational modeling is achievable through refinement of modeling.

## References


1. Ludmila Novakova-Marcincinova, Ivan Kuric: "Basic and Advanced Materials for Fused Deposition Modeling Rapid Prototyping Technology," Manuf. and Ind. Eng., 11(1), 25–27 (2012), ISSN 1338–6549.
2. Water C. Smith and Richard W. Dean: "Structural Characteristics of Fused Deposition Modeling Polycarbonate Material," Polymer Testing, 32(8), 1306–12 (2013).
3. Joseph E. Grady, William J. Haller, Phil Poinsatte, Michael C. Halbig, Sydney Schulo, M. Singh, Don Weir, Natalie Wali, Michael Vinup, Michael G. Jones, Clark Patterson, and Tom Santelle, "A Fully Non-Metallic Gas Turbine Engine Enabled by Additive Manufacturing: *Part I: System Analysis, Component Identification, Additive Manufacturing, and Testing of Polymer Composites*," NASA TM-2015-218748 Glenn Research Center, Cleveland, OH (2015).
4. Angnes Bagsik and Volker Shoppner: "Mechanical Properties of Fused Deposition Modeling Parts Manufactured with Ultem 9085," ANTEC Conference Proceedings, May 1–5, Boston, MA (2011).
5. A. Sherif El-Gizawy, Joseph Cardona, Brian Graybill: "An Integrated Approach for Characterization of Properties and Mesostructure of Fused Deposition Modeling Ultem 9085 Products," SAMPE Conference Proceedings, 55, May 17–20, Seattle, WA (2010).
6. America Makes contract report (2014): "Maturation of Fused Deposition Modeling (FDM) Component Manufacturing (4003)," by Rapid Prototype Plus Manufacturing (rp+m).